General Incident Angle Modifier Model for Quasi-Dynamic Testing of Solar Thermal Collectors

J. M. Rodríguez-Muñoz, I. Bove and P. Galione

Laboratorio de Energía Solar, Universidad de la República (Uruguay)

Abstract

The thermal performance of solar collectors is commonly evaluated using standardized procedures, with ISO 9806 being the most widely applied. This standard defines two testing methods: steady-state testing (SST) and quasi-dynamic testing (QDT). While SST requires clear-sky conditions, QDT allows testing under variable weather conditions but introduces challenges in modelling the incident angle modifier (IAM) for beam radiation. Several IAM models have been proposed within the framework of the QDT method, yet no consensus exists on the most suitable one, leading laboratories to rely on empirical choices for each specific technology, which compromises result comparability. To address this limitation, a general IAM model was recently proposed and successfully applied to both flat-plate and evacuated tube collectors, improving accuracy across a wide range of incidence angles, though at the cost of an increased number of fitting parameters. This paper builds upon that work by evaluating the model's applicability to evacuated tube collectors with CPC reflectors and by performing a sensitivity analysis of the angular discretization step, which directly influences the number of fitting parameters. The results show that the model is suitable for application to this technology, advancing its general applicability, and that an angular step of 10°, as recommended by ISO 9806, is sufficient to accurately represent IAM curves for evacuated tube collectors while limiting the number of fitting parameters and maintaining manageable parameter identification procedure.

Keywords: solar thermal collectors, incident angle modifier, ISO 9806.

1. Introduction

Solar thermal systems are used in a wide range of applications, including domestic hot water production, space heating and cooling, industrial process heat, and electricity generation. Their core component — the solar thermal collector — captures solar energy and transfers it to a working fluid, making its thermodynamic characterization a key aspect of solar thermal energy system evaluation. Standardized tests are commonly employed for this purpose, with ISO 9806 (2017) being the most widely adopted standard. This standard defines two test methods: Steady-State Testing (SST) and Quasi-Dynamic Testing (QDT). The SST method requires clear skies and stable inlet fluid conditions, whereas the QDT method accounts for dynamic effects and enables testing under cloudy conditions. This flexibility allows for more frequent testing in variable weather, but also introduces additional challenges, particularly in modelling the Incident Angle Modifier (IAM) for beam solar radiation.

The Incidence Angle Modifier (IAM) for beam solar radiation depends on the angle of incidence, and several models have been proposed within the QDT framework. Each model includes a set of parameters that must be determined from experimental data, some of which have a direct physical meaning, while others do not. The traditional model developed for flat-plate collectors (Souka & Safwat, 1966), although very simple to implement as it involves only one fitting parameter, often fails to accurately represent experimental results (Rodríguez-Muñoz et. al, 2021). Alternative formulations (Sallaberry et al., 2011; Zambolin & Del Col, 2012; Osório & Carvalho, 2014) have not consistently shown better performance. A similar lack of consensus exists for evacuated tube collectors. In particular, this type of technology exhibits highly diverse and complex IAM curves, requiring a larger number of fitting parameters. In such cases, the shape of the IAM depends on the geometry of the absorber inside the tubes and on whether or not compound reflectors are used. Consequently, test users must currently select an IAM model for each collector technology based on their own experience.

10.18086/swc.2025.02.15 Available at http://proceedings.ises.org

This reveals a clear research gap: a general model applicable to different technologies would strengthen the robustness of the QDT method by reducing tester dependence and ensuring consistent performance.

Rodríguez-Muñoz et al. (2021) proposed a novel formulation to address this research gap. This approach generalizes the SST method by discretizing the range of incidence angles into sub-intervals and representing the IAM as a piecewise linear function. For instance, with an angular step of 10°, the model parameters correspond to the IAM values at angles from 0° to 90° in 10° increments, giving the fitting parameters a clear physical meaning—an advantage over other models. The model improves IAM accuracy across a wide range of incidence angles, and representing the IAM through discrete angular intervals provides a flexible and robust framework, as various experimental curves can be approximated by linear segments defined through nodal values at fixed angle steps, making the model easily adaptable to different technologies. In this sense, the model has been experimentally validated for flat-plate collectors and for evacuated tube collectors with heat pipes (Rodríguez-Muñoz et al., 2021; 2024). For evacuated tube technology, the commonly used assumption of IAM factorization is adopted, and the discretization procedure is applied independently to both the longitudinal and transversal components. The main drawback of this approach is the increased number of fitting parameters, which depends on the selected angular step.

Building on these previous works, the present study applies the proposed model to an evacuated tube collector with CPC reflectors, tested using the Quasi-Dynamic Testing (QDT) method at the Solar Energy Laboratory in Uruguay, further demonstrating the model's adaptability to different IAM curve shapes. Previous test results of the same collector without CPC were available for comparison. Additionally, a sensitivity analysis of the angular step was performed, showing that a 10° interval is sufficient to accurately describe the IAM curves of evacuated tube collectors, both with and without CPC reflectors, while limiting the total number of fitting parameters and simplifying the parameter identification procedure.

This article is organized as follows: Section 2 outlines the thermodynamic and novel IAM model; Section 3 presents the test facility and methodology; Section 4 discusses the results; and Section 5 summarizes the main conclusions of the study.

2. Thermodynamic model and general indecent modifier model

2.1. Standard thermodynamic model

The ISO 9806:2017 standard defines a general thermal model applicable to various types of solar thermal collector technologies. Depending on the specific collector design, certain terms and coefficients in the model may be neglected. Eq. (1) presents the thermal model for low-temperature collectors with a cover.

$$\frac{\dot{Q}_u}{A_G} = \eta_{0,b}.\left[K_b(\theta).G_b + K_d.G_d\right] - a_1(\vartheta_m - \vartheta_a) - a_2(\vartheta_m - \vartheta_a)^2 - a_5\frac{d\vartheta_m}{dt}\,, \qquad \text{(eq. 1)}$$

where G_b and G_d are the direct and diffuse solar irradiance on the collector plane, respectively; ϑ_m is the mean temperature of the working fluid (the average of the inlet, ϑ_i, and outlet, ϑ_o, temperatures); and ϑ_a is the ambient air temperature. The characteristic parameters are: $\eta_{0,b}$, $K_b(\theta)$, K_d, a_1, a_2, and a_5. The first three are related to the optical efficiency; a_1 and a_2 represent heat loss coefficients; and a_5 is the effective thermal capacity divided by the gross collector area (A_g).

2.2. Incident angle modifier (IAM)

All parameters presented in the above section are assumed to be constant, except for the incidence angle modifier for direct solar irradiance, $K_b(\theta)$, which varies with the angle of incidence. This function describes the variation of the collector's optical efficiency relative to normal incidence as a function of the incidence angle and is typically represented by an empirical expression with adjustable parameters.

The novel model involves dividing the incident angle range into smaller intervals and assuming a piecewise linear function within each interval, taking the nodal values of the IAM as parameters to be determined. For instance, if a 10° interval is employed, the adjustable parameters would be $K_b(10°)$, $K_b(20°)$, …, $K_b(80°)$, where $K_b(\theta_i)$ represents the K_b value at the angle θ_i (or node). Then the K_b value for any θ angle can be expressed as:

$$K_b(\theta) = K_b\left(\left\lfloor\frac{\theta}{10}\right\rfloor 10\right)\left(\left\lfloor\frac{\theta+10}{10}\right\rfloor - \frac{\theta}{10}\right) + K_b\left(\left\lfloor\frac{\theta}{10}\right\rfloor 10 + 10\right)\left(\frac{\theta}{10} - \left\lfloor\frac{\theta}{10}\right\rfloor\right), \quad \text{(eq. 2)}$$

where the open square brackets indicate to round up to the previous lower natural number. For all types of collectors, it is mandated that $K_b(0°) = 1$ and $K_b(90°) = 0$ for the first and last parameters, respectively.

For evacuated tube collectors, K_b depends on two incidence angles: θ_L (longitudinal) and θ_T (transverse), i.e. $K_b(\theta_L,\theta_T)$. A common simplification, introduced by McIntire (1982), factorizes K_b as the product of two independent functions, $K_b=K_{bL}\times K_{bT}$, where K_{bL} and K_{bT} represent the IAM evaluated at (θ_L, θ_T=0°) and (θ_L=0°, θ_T), respectively. This factorization is widely adopted in performance testing. In this study, the same factorization was adopted, applying the discretization proposed by Rodríguez-Muñoz et al. (2021) to both K_{bL} and K_{bT} function.

2.3. Parameter identification procedure

Two parameter identification approaches are available for the QDT method (Fischer et al., 2004), differing in how they handle transient effects. The first, known as Multi-Linear Regression (MLR) (Perers, 1997), approximates the time derivative using finite differences and includes it as an independent variable. The second, Dynamic Parameter Identification (DPI), performs a dynamic simulation coupled with a non-linear regression algorithm. Although more complex, the DPI approach more accurately captures transient collector behavior under both standard and in-situ conditions (Hofer et al., 2015; Fahr et al., 2016) and is particularly suitable for ETC-HP technology (Rodríguez-Muñoz et al., 2025). In this study, the DPI method was adopted due to its higher reliability and suitability, complementing the precision of the proposed IAM model. A MATLAB tool was developed in the framework of a previous work, to facilitate its implementation, which can be download here: https://bit.ly/STCT-Program-V3.

3. Experimental data and methodology

3.1. Test facilities and solar collector tested

In this study, an evacuated tube solar thermal collector with heat pipes and CPC reflectors, with a gross area of 1.79 m², was tested at the Solar Heaters Test Platform (BECS) within the Solar Energy Laboratory (LES, http://les.edu.uy/) of the Universidad de la República (UdelaR) between February and March 2025. The facility is located near the city of Salto, Uruguay (latitude: 31.28° S, longitude: 57.92° W), and the test installation complies with all the requirements of ISO 9806 (2017). Figure 1 shows the assembly of the collector without CPC reflectors on the test bench for illustrative purposes.

Figure 1: Assembly of the collector on the solar tracker of the test bench, figure extracted from Rodríguez-Muñoz et. al. 2024.

The collector has a standardized design, incorporating borosilicate glass tubes with an outer diameter of 59 mm and a length of 1.80 m. It includes eight heat pipes with cylindrical metal fin absorbers of 47 mm, spaced 52 mm apart. Each heat pipe measures 168.7 cm in total length, with 163 cm allocated to the evaporator section and 5.7 cm to the condenser section. The condenser and evaporator have diameters of 14 mm and 8 mm, respectively. A stainless-steel compound parabolic concentrator (CPC) is integrated into the design, with a concentration ratio of C=0.75.

3.2. Methodology

The tests followed the QDT methodology of ISO 9806 (2017), and the test data were averaged every minute. The parameters of the thermodynamic models described in Eqs. (1) and (2) were determined using the DPI procedure. Previous tests of the same solar collector without CPC reflectors were available for comparison (Rodríguez-Muñoz et al., 2024); however, in this study, those data were reprocessed using the same averaging interval and parameter identification procedure to ensure a more consistent and reliable comparison.

It should be noted that annual tests have been performed on a reference collector since 2019 as a quality assurance practice to verify the proper operation and long-term stability of the testing platform. This procedure ensures the comparability of test results obtained over time. The reference collector consists of a flat-plate collector that was used in an interlaboratory comparison conducted in the Latin American region and organized by the German Metrology Institute (PTB, for its name in German), during which our testing platform was validated using both testing methods (Fischer, 2020).

In the next section, the test results are first presented using an angular step of 10°, which corresponds to the standard value, as the standard requires presenting nodal values in 10° increments. Then, smaller angular steps were evaluated to assess the impact of this variable on the shape of the IAM curve. For each angular step, the root mean square deviation (RMSD) was calculated to evaluate its influence on the power output of the collector, according to Eq. (3):

$$RMSD = \left[\frac{1}{n}\sum_{i=1}^{n}(\hat{y}_i - y_i)^2\right]^{1/2}, \qquad \text{(eq. 3)}$$

where y_i represents the reference value (measured useful power produced by the collector), $\hat{y}_i$ is the model estimate (useful power given by Eqs. (1) and (2) and the fitted parameters), and n is the total number of measurements. For a better comparison between collectors and to provide a more consistent framework in general, the relative value with respect to the mean measured useful power, $\langle \dot{Q}_u \rangle$, is reported, that is,

$$rRMSD = \frac{RMSD}{\langle \dot{Q}_u \rangle}. \qquad \text{(eq. 4)}$$

This performance indicator is presented for three cases: (i) considering all data used for fitting, (ii) considering only the data corresponding to the parameter identification of K_{bL}, and (iii) considering only the data corresponding to the parameter identification of K_{bT}. Cases (ii) and (iii) correspond to measurement sequences with an average fluid temperature close to ambient, under clear-sky conditions. Case (ii), related to K_{bL}, is conducted with azimuthal solar tracking so that $K_{bT} = 1$, while case (iii), related to K_{bT}, is performed with the tracker fixed to the north and a horizontal inclination such that $K_{bT} \approx 1$.

4. Results

4.1. Parameter identification

Table 1 shows the parameter values of the thermodynamic models from Eqs. (1) and (2). Uncertainties are reported only when required by the standard (i.e., for performance parameters — all except those related to the beam IAM) to simplify the table for both configurations, with and without CPC reflectors. In all cases, a *t*-ratio greater than two was obtained (i.e., the ratio between each parameter value and its corresponding uncertainty), indicating statistical significance for all parameters.

Figure 2 graphically presents the IAM, specifically the functions $K_{bL}$and K_{bT}as a function of the incidence angle. The values at high incidence angles correspond to linearly interpolated points between the largest measured angle and 90°, a common practice to obtain a complete representation of these functions over the entire range of incidence angles.

The behavior observed in these figures is consistent with what is expected for this type of collector (Zambolin & Del Col, 2012). The function K_{bL}decreases monotonically over the entire range in both cases. For K_{bT}, in the configuration without CPC reflectors, the function increases and reaches a maximum value around 70°, after which it decreases sharply. When the CPC is included, K_{bT} first decreases up to about 40°, then increases until approximately 70°, reaching a similar maximum but of lower magnitude, and finally decreases again. As expected, the inclusion of the CPC increases peak efficiency while reducing the nodal values of K_{bT}. The consistency of these results with previous studies further supports the applicability of the proposed model to this specific collector technology.

Tab. 1: Value and uncertainty of the characteristic parameters of each case, with and without CPC.

	With CPC		Without CPC	
	Value	Uncertainty	Value	Uncertainty
$\eta_{0,b}$	0.415	± 0.0004	0.262	± 0.0003
K_d	1.201	± 0.006	1.252	± 0.005
a_1(W/m^2.K)	0.762	± 0.019	1.09	± 0.023
a_2(W/m^2.K^2)	0.004	± 0.0002	0.003	± 0.0003
a_5 (kJ/K.m^2)	115	± 0.7	85.7	± 1.0
θ_L / θ_T	K_{bL}	K_{bT}	K_{bL}	K_{bT}
0	1.00	1.00	1.00	1.00
10	0.99	0.99	1.00	1.03
20	1.00	0.95	1.00	1.08
30	1.00	0.95	1.00	1.15
40	1.00	0.92	1.00	1.34
50	0.80	1.02	1.00	1.59
60	0.60	1.39	0.75	2.12
70	0.40	1.44	0.50	2.38
80	0.20	0.72	0.25	1.19
90	0	0	0	0

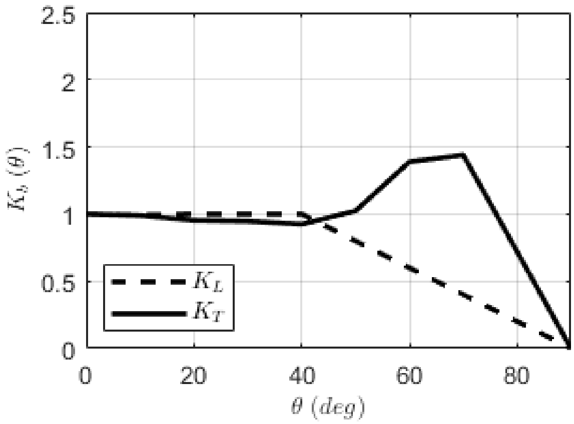

Figure 1a: Collector with CPC.

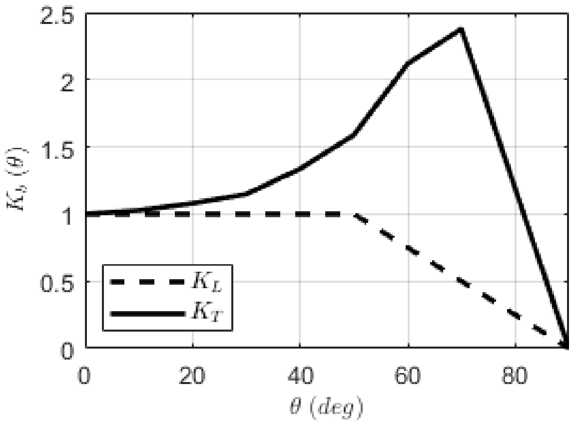

Figure 1a: Collector without CPC.

Figure 2: Graphical representation incident angle modifier for beam irradiance for both collectors.

4.2. Angular step analysis

Figure 3 shows the relative root mean square deviation (rRMSD) for different angular steps, ranging from 2° to 10° in increments of 2°, for the three cases described in the previous section. For both collectors and all cases considered, the error remains fairly uniform across the range considered and is below 3% in all cases. In particular, for the collector with CPC reflectors, the error is below 2%.

During the analysis, IAM curves similar to those in Figure 2 were also examined for the different cases (not shown here), revealing very similar shapes but smoother transitions—especially around the maximum point, which appears to occur at a slightly lower incidence angle than 70°, close to the angle at which the tubes begin to cast shadows on each other (approximately 63°).

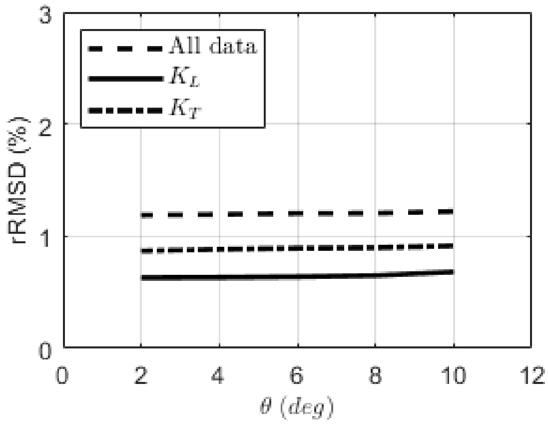

Figure 1a: Collector with CPC.

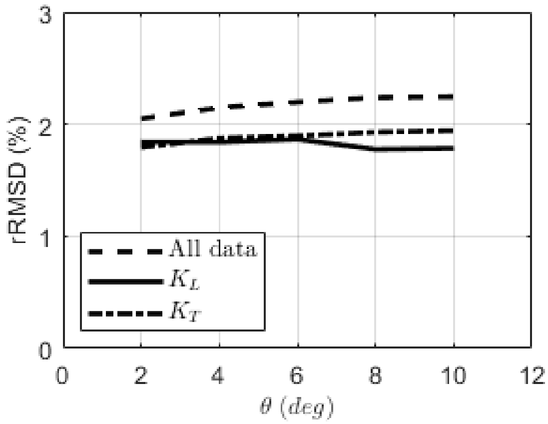

Figure 1a: Collector without CPC.

Figure 3: rRMSD as a function of the discretization step angle for the IAM. The mean useful power corresponds to 360 W/m² and 234 W/m² for the collector with and without CPC reflectors, respectively.

In conclusion, although a smaller angular step allows for smoother and more accurate IAM curves, this does not translate into a significant reduction in the error associated with useful power. Therefore, using angular steps smaller than 10° does not appear necessary, as it provides no additional advantages and unnecessarily increases the number of parameters, which complicates the parameter identification procedure.

5. Conclusions

The novel Incident Angle Modifier (IAM) model, originally developed for flat-plate collectors and later extended to evacuated tube collectors without CPC reflectors, has now been successfully applied to an evacuated tube collector with CPC reflectors within the framework of the Quasi-Dynamic Testing (QDT) method. This approach generalizes the Steady-State Testing (SST) method by discretizing the range of incidence angles into sub-intervals and representing the IAM as a piecewise linear function. The fitting parameters correspond directly to the nodal IAM values at discrete angles, giving them clear physical meaning. For ETC collectors, the model adopts the standard IAM factorization into longitudinal and transversal components, applying the discretization procedure independently to each. Its successful application to ETCs with CPC reflectors represents a step forward in the model's general applicability across different collector technologies.

While this approach enhances IAM accuracy across a wide range of incidence angles compared to simpler models, its main drawback is the increased number of fitting parameters. To assess the impact of angular discretization—which directly determines the number of fitting parameters—a sensitivity analysis was performed using angular steps from 2° to 10° in increments of 2°, with a 10° step being the one recommended by the ISO 9806 standard. The results showed that the relative root mean square deviation (rRMSD) of the calculated useful power remained fairly uniform across the analyzed range, staying below 3% in all cases and below 2% for the collector with CPC reflectors. Although smaller angular steps yield smoother and more precise IAM curves, they do not lead to a significant reduction in the useful power error. Therefore, an angular step of 10° is the most convenient choice, as it provides a good representation of the IAM curve while limiting the number of fitting parameters.

6. Acknowledgments

The authors gratefully acknowledge the National Agency of Research and Innovation (ANII) of Uruguay for its financial support through project ANII_ART_X_2023_1_179571 “Calor y acumulación solar para la industria”, within the framework of which the CPC reflector used in this work was constructed.

7. References

Fahr, S., Gumbel, U., & Zirkel-Hofer, A. (2018). *In situ characterization of thermal collectors in field installations*. In *Proceedings of EuroSun 2018*. https://doi.org/10.18086/eurosun2018.12.01

Fischer, S., Heidemann, W., Müller-Steinhagen, H., Perers, B., Bergquist, P., & Hellström, B. (2004). Collector test method under quasi-dynamic conditions according to the European standard EN 12975-2. *Solar Energy, 76*(1), 117–123. https://doi.org/10.1016/j.solener.2003.07.021

Fischer, S. (2020). Quality Infrastructure for Energy Efficiency and Renewable Energy in Latin America and the Caribbean, Report # 95309. Report Intituto Metrológico Aleman - PTB.

Hofer, A., Büchner, D., Kramer, K., Fahr, S., Heimsath, A., Platzer, W., & Scholl, S. (2015). Comparison of two different (quasi-) dynamic testing methods for the performance evaluation of a linear Fresnel process heat collector. *Energy Procedia, 69*, 84–95. https://doi.org/10.1016/j.egypro.2015.03.011

ISO 9806. (2017). *Solar energy – Solar thermal collectors – Test methods*. International Organization for Standardization.

McIntire, W. R. (1982). Factored approximations for biaxial incident angle modifiers. *Solar Energy, 29*, 315–322. https://doi.org/10.1016/0038-092X(82)90246-8

Osório, T., & Carvalho, M. J. (2014). Testing of solar thermal collectors under transient conditions. *Solar Energy, 104*, 71–81. https://doi.org/10.1016/j.solener.2014.01.048

Perers, B. (1997). An improved dynamic solar collector test method for determination of non-linear optical and thermal characteristics with multiple regression. *Solar Energy, 59*(4), 163–178. https://doi.org/10.1016/S0038-092X(97)0147-3

Rodríguez-Muñoz, J. M., Bove, I., & Alonso-Suárez, R. (2021). Novel incident angle modifier model for quasi-dynamic testing of flat plate solar thermal collectors. *Solar Energy, 224*, 112–124. https://doi.org/10.1016/j.solener.2021.05.026

Rodríguez-Muñoz, J. M., Bove, I., & Alonso-Suárez, R. (2024). Improving the experimental estimation of the incident angle modifier of evacuated tube solar collectors with heat pipes. *Renewable Energy, 235*, 121240. https://doi.org/10.1016/j.renene.2023.121240

Rodríguez-Muñoz, J. M., Bove, I., Alonso-Suárez, R., & Galione, P. (2025). On the choice of the parameter identification procedure in quasi-dynamic testing of low-temperature solar collectors. *Renewable Energy, 247*, 122931. https://doi.org/10.1016/j.renene.2025.122931

Sallaberry, F., García de Jalón, A., Olano, X., Mateu, E., Erice, R., & Ramirez, L. (2011). Bi-axial incidence angle modifier using quasi-dynamic test for asymmetrical solar collector using dummy variables. In *ESTEC Congress*, Marseille, France.

Souka, A., & Safwat, H. (1966). Determination of the optimum orientations for the double-exposure, flat-plate collector and its reflectors. *Solar Energy, 10*(4), 170–174. https://doi.org/10.1016/0038-092X(66)90004-1

Zambolin, E., & Del Col, D. (2012). An improved procedure for the experimental characterization of optical efficiency in evacuated tube solar collectors. Renewable Energy, 43, 37 – 46. doi: https://doi.org/10.1016/j.renene.2011.11.011.734